Pure appl. geophys. 164 (2007) 1985–2007
0033–4553/07/101985–23
DOI 10.1007/s00024-007-0259-7

Pure and Applied Geophysics

Crust and Upper Mantle Structure in the Caribbean Region by Group Velocity Tomography and Regionalization

O'LEARY GONZÁLEZ,[1,2] LEONARDO ALVAREZ,[1,2] MARIANGELA GUIDARELLI,[3] and GIULIANO F. PANZA[2,3]

Abstract—An overview of the crust and upper mantle structure of Central America and the Caribbean region is presented as a result of the processing of more than 200 seismograms recorded by digital broadband stations from SSSN and GSN seismic networks. Group velocity dispersion curves are obtained in the period range from 10s to 40s by FTAN analysis of the fundamental mode of the Rayleigh waves; the error of these measurements varies from 0.06 and 0.09 km/s.From the dispersion curve, seven tomographic maps at different periods and with average spatial resolution of 500 km are obtained. Using the logical combinatorial classification techniques, eight main groups of dispersion curves are determined from the tomographic maps and eleven main regions, each one characterized by one kind of dispersion curves, are identified. The average dispersion curves obtained for each region are extended to 150s by adding data from a larger-scale tomographic study (VDOVIN *et al.*, 1999) and inverted using a nonlinear procedure. A set of models of the S-wave velocity vs. depth in the crust and upper mantle is found as a result of the inversion process.In six regions we identify a typically oceanic crust and upper mantle structure, while in the other two the models are consistent with the presence of a continental structure. Two regions, located over the major geological zones of the accretionary crust of the Caribbean region, are characterized by a peculiar crust and upper mantle structure, indicating the presence of lithospheric roots reaching, at least, about 200 km of depth.

Key words: Surface waves tomography, group velocities dispersion curves, S-wave velocity models, Caribbean region, regionalization.

Introduction

The Caribbean region comprises the sea with the same name, an island arc and continental portions of Central and South America. This region is mainly characterized by oceanic crust with great heterogeneities that reveal its complex geology. There are important tectonic elements as the Cayman Trough (where a

[1] Centro Nacional de Investigaciones Sismológicas, Ministerio de Ciencia, Tecnología y Medio Ambiente, Cuba. Calle 17 # 61. Rpto. Vista Alegre, Santiago de Cuba, Cuba 90400.
E-mail: oleary@cenais.ciges.inf.cu
[2] The Abdus Salam International Centre for Theoretical Physics, Earth System Physics section, Strada Costiera 11, Trieste 34014, Italy.
[3] Department of Earth Sciences, University of Trieste, Via Weiss 4, Trieste, Italy.

process of formation of oceanic crust is in progress), the Cayman Ridge and Gonave microplate, as well as zones with accretionary crust (where the North American plate is subducting beneath the Caribbean plate, and the Nazca and Cocos plates are subducting beneath the Caribbean and North American plates, Fig. 1). A detailed analysis of the geological and tectonic characteristics of this region can be found in DENGO and CASE (1990).

Pioneering studies of the dispersion of group velocity of Rayleigh waves in the region that includes the Caribbean, Central America, Central Western Atlantic Ocean and the Northern part of South America were performed in the sixties (PAPAZACHOS, 1964; TARR, 1969) and in Cuba somewhat later (ALVAREZ, 1977).

In recent years, the existence of specific software for data processing and inversion and of broadband stations (BB) with digital recording in the area has increased the quality of the available dispersion measurements. In an earlier paper (GONZALEZ *et al.*, 2000) group velocity dispersion curves for fundamental mode Rayleigh waves were determined along several paths and inverted to obtain crust-upper mantle models. The availability of data for the crust structure, summarized and generalized by several authors, (e.g., DENGO and CASE, 1990; VAN DER HILST, 1990), the most recent regional studies (VDOVIN *et al.*, 1999; BASSIN *et al.*, 2000; CHULICK and HOONEY, 2002; LIGORRÍA and MOLINA, 1997; MORENO *et al.*, 2002; PINDELL and KENNAN, 2001) and global studies (LASKE and MASTERS, 1997; MONTAGNER and KENNET, 1996; MOONEY *et al.*, 1998) allow us now to make a refined study of the region. For this purpose we perform Rayleigh wave group velocity tomography, considering relatively short paths (regional trajectories), we regionalize the dispersion curves locally obtained by the tomography and we invert them into average regionalized structural models with a nonlinear inversion scheme.

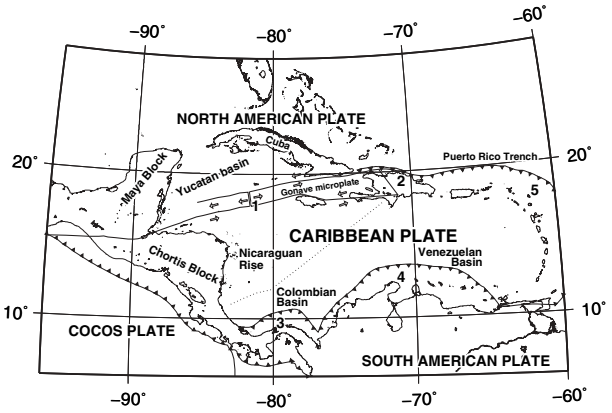

Figure 1
Schematic map of Caribbean region. (1. Cayman Trough, 2. Greater Antilles deformed belt, 3. North Panama deformed belt, 4. South Caribbean deformed belt and 5. Lesser Antilles deformed belt.).

Data

The primary selection of waveforms to be used in the dispersion analysis has been done in the World Data Center (IRIS) and in the archives of the Cuban National Seismological Service (SSSN), imposing the following criteria on the source properties:

Depth: $h < 75$ km, Magnitude: $M_S > 5.0$, Latitude (North): 0°–35°, Longitude (West): 50°–120°. As a result 205 records, obtained at 13 broadband regional stations (Table 1), have been processed and the corresponding dispersion curves have been obtained in the period range from 10 s to 40 s (LEVSHIN *et al.*, 1999). The upper period limit is imposed by the technical characteristics of the BB stations of the Cuban National Seismological Service (ZAPATA *et al.*, 2001), which recorded the largest number of seismograms. The stations, epicenters and paths are shown in Figure 2.

The Method

a) Determination of Dispersion Curves and Tomographic Maps

The dispersion curves of the fundamental mode of Rayleigh waves along each path are determined using the frequency-time analysis (FTAN) in its most updated version (LEVSHIN *et al.*, 1972, 1992). Appendix 1 shows an example of dispersion curves determined from the original seismogram by FTAN procedure and the

Table 1

Code, region, latitude, longitude and elevation of the stations, which have recorded the events selected for surface wave tomography. SSSN – Sistema del Servicio Sismológico Nacional (Cuba), GSN – Global Seismic Network

Station code	Region	Latitude (°N)	Longitude (°W)	Elevation (m)	Network
RCC	Río Carpintero	19.9942	−75.6958	100.0	SSSN
CCCC	Cascorro	21.2000	−77.7660	150.0	SSSN
LMGC	Las Mercedes	20.0640	−77.0050	220.0	SSSN
MOAC	Moa	20.6600	−74.9600	120.0	SSSN
MASC	Maisí	20.1750	−74.2310	320.0	SSSN
MGV	Manicaragua	22.1100	−79.9800	300.0	SSSN
SOR	Soroa	22.7840	−83.0080	206.0	SSSN
DWPF	Disney Wilderness Preserve	28.1103	−81.4328	142.4	GSN
HKT	Hockley	29.9500	−95.8333	415.0	GSN
SDV	Santo Domingo	8.8861	−70.6333	1580.0	GSN
TEIG	Tepich	20.2263	−88.2764	69.0	GSN
SJG	San Juan (Cayey)	18.1117	−66.1500	457.0	GSN
JTS	Juntas de Abangares	10.2908	−84.9525	340.0	GSN

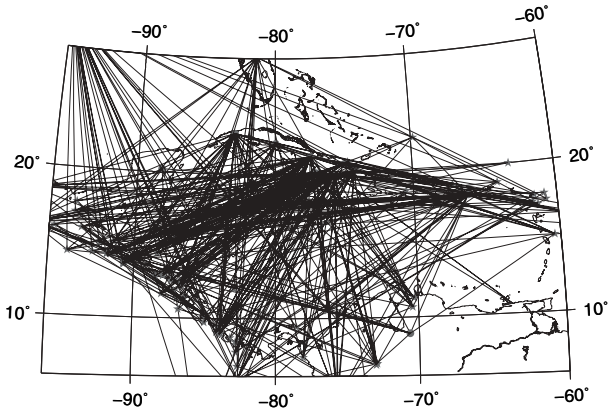

Figure 2
Epicenters (stars), stations (black points) and seismic paths selected for surface-wave tomography.

Rayleigh surface waves filtered. The experimental errors of these measurements for each period range from 0.06 to 0.09 km/s are determined as the average between the differences of group velocity values for at least 5 pair of paths, where for each pair the station is the same and the distance between the epicenters is less than 0.3° (Table 2).

A ray tomography analysis method, which is described in DITMAR and YANOVSKAYA (1987), YANOVSKAYA and DITMAR (1990), WU and LEVSHIN (1994), and YANOVSKAYA (1997), and is the generalization of the one-dimensional inversion method of BACKUS and GILBERT (1968, 1970) for 2-D problems is applied to the dispersion curves, with a smoothness criteria described by YANOVSKAYA and DITMAR (1990). A set of seven tomographic maps for periods ranging from 10 s to 40 s at intervals of 5 s is obtained (Fig. 3). The resolution of the results depends on the coverage of the region by the paths epicenter-station and on its azimuthal distribution. At each point the lateral resolution (a), which is determined by the density of paths, is about 500 km in the Central-West Caribbean, the Antilles and south of Central America (Fig. 4). The stretching parameter (ex) in general indicates how adequate (uniform) the spatial distribution of paths is. Small values of ex (≤ 0.5) indicate that the obtained solution is locally smoothed over an area of the same size in all directions. Large values of ex (≥ 1) indicate that a preferred orientation of the paths exists and for this reason the tomographic study provides no additional information with respect to the original data relative to the paths. Figure 5 shows the distribution of parameter ex, which is adequate in the area where the lateral resolution is better than 500 km. As could be expected, due to the inclusion of relatively more local dispersion paths,

Table 2

Experimental errors determined from the measurements of group velocity for each period

Period (s)	Group velocity km/s)										Measurement error (km/s)
	Station CCCC		Station DWPF		Station SJG		Station RCC		Station SOR		
	Event 1	Event 2	Event 1	Event 2	Event 1	Event 2	Event 1	Event 2	Event 1	Event 2	
10	2.74	2.92	2.69	2.32	3.04	3.08	2.26	2.41	2.88	2.69	±0.09
15	2.99	2.95	2.70	2.62	3.04	3.08	2.53	2.44	3.34	2.80	±0.08
20	3.03	3.05	2.85	2.81	3.11	3.13	3.01	2.89	3.60	3.19	±0.06
25	3.25	3.25	3.10	3.03	3.28	3.32	3.49	3.32	3.71	3.40	±0.06
30	3.44	3.38	3.35	3.25	3.38	3.44	3.58	3.51	3.79	3.52	±0.06
35	3.57	3.51	3.51	3.52	3.51	3.51	3.61	3.59	4.20	3.70	±0.06
40	3.65	3.60	3.63	3.62	3.55	3.55	3.74	3.63	4.04	3.64	±0.06

the lateral resolution that we obtain is better than the one obtained by VDOVIN *et al.* (1999) for the same area.

b) Regionalization Analysis of Tomography Results

Considering their lateral resolution, the tomographic maps are discretized in cells of $2^\circ \times 2^\circ$ and for each one dispersion curves are determined. A discrimination based on tomography resolution over the original 200 ($2^\circ \times 2^\circ$) cells is done and only those cells belonging to the areas where the lateral resolution is ≤ 500 km have been selected. They essentially correspond to a region that comprises Central-Eastern Caribbean, Central America and the northernmost part of Western Venezuela and Colombia. For each of the 81 selected cells, a group velocity dispersion curve is constructed. Their visual inspection evidences the presence of regions with an approximately similar dispersion.

To spatially delimit such regions, the grouping of the dispersion curves is performed using an extension of the non-supervised logical-combinatorial algorithms included in PROGNOSIS system (RUIZ *et al.*, 1992; PICO, 1999). The main characteristics of the algorithm are the following:

- Let the grid point number j be the object O_j. An object is described in terms of the variables $x_t(O_j)$, $t = 1, n$. In our case, the variables are the values of the group velocity at different periods.
- Let C_t be the comparison criterion between two objects for the variable "x_t", defined as:

$$C_t\left[x_t(O_i), x_t\left(O_j\right)\right] = \begin{cases} 1 & \text{if} \quad \left|x_t(O_\mathrm{i}) - x_t(O_j)\right| \leq \varepsilon_t \\ 0 & \text{elsewhere} \end{cases} \tag{1}$$

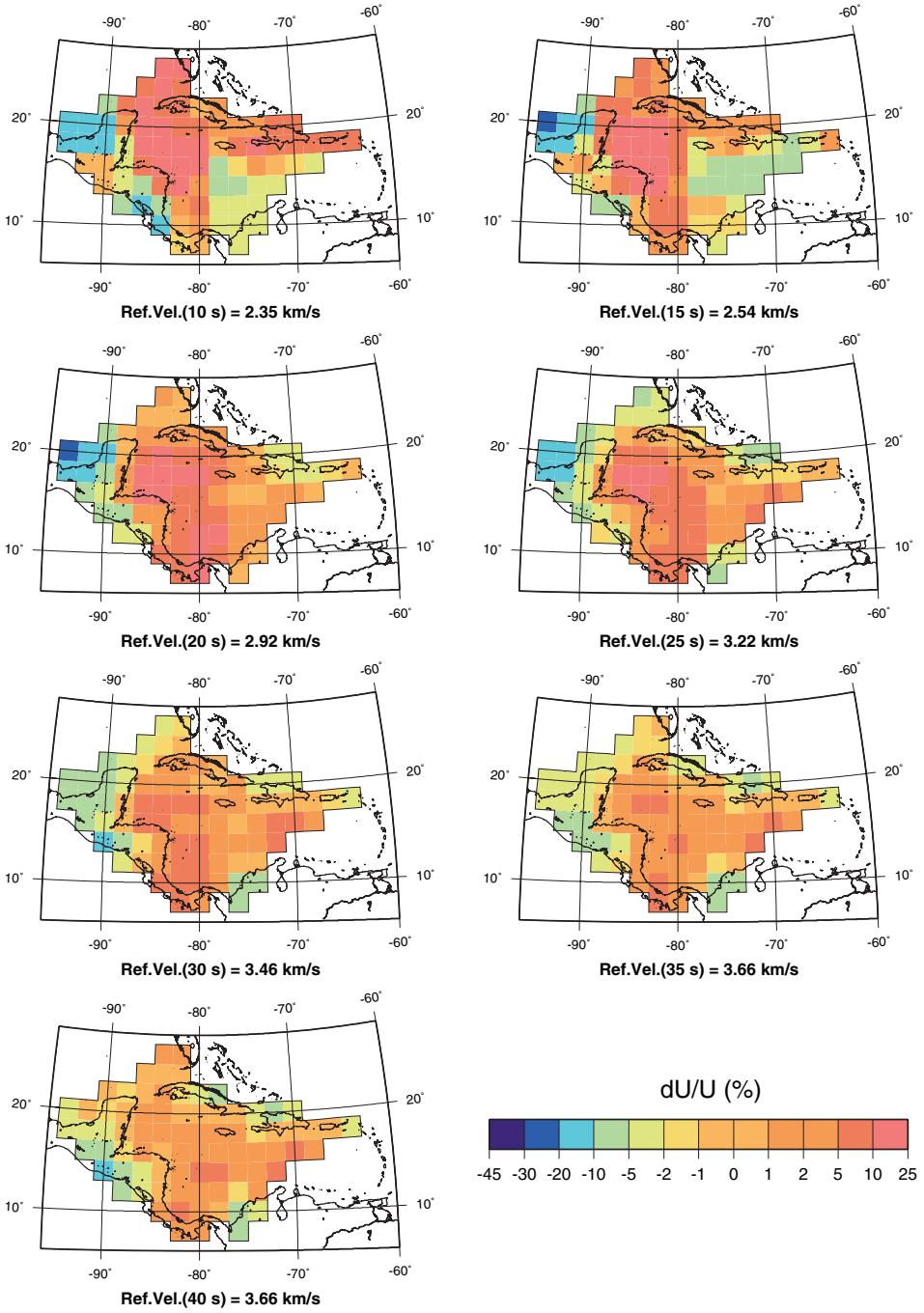

Figure 3
Rayleigh waves group velocity tomography at different periods (10–40 s) shown as percent deviation from the average reference velocity (Ref. Vel.).

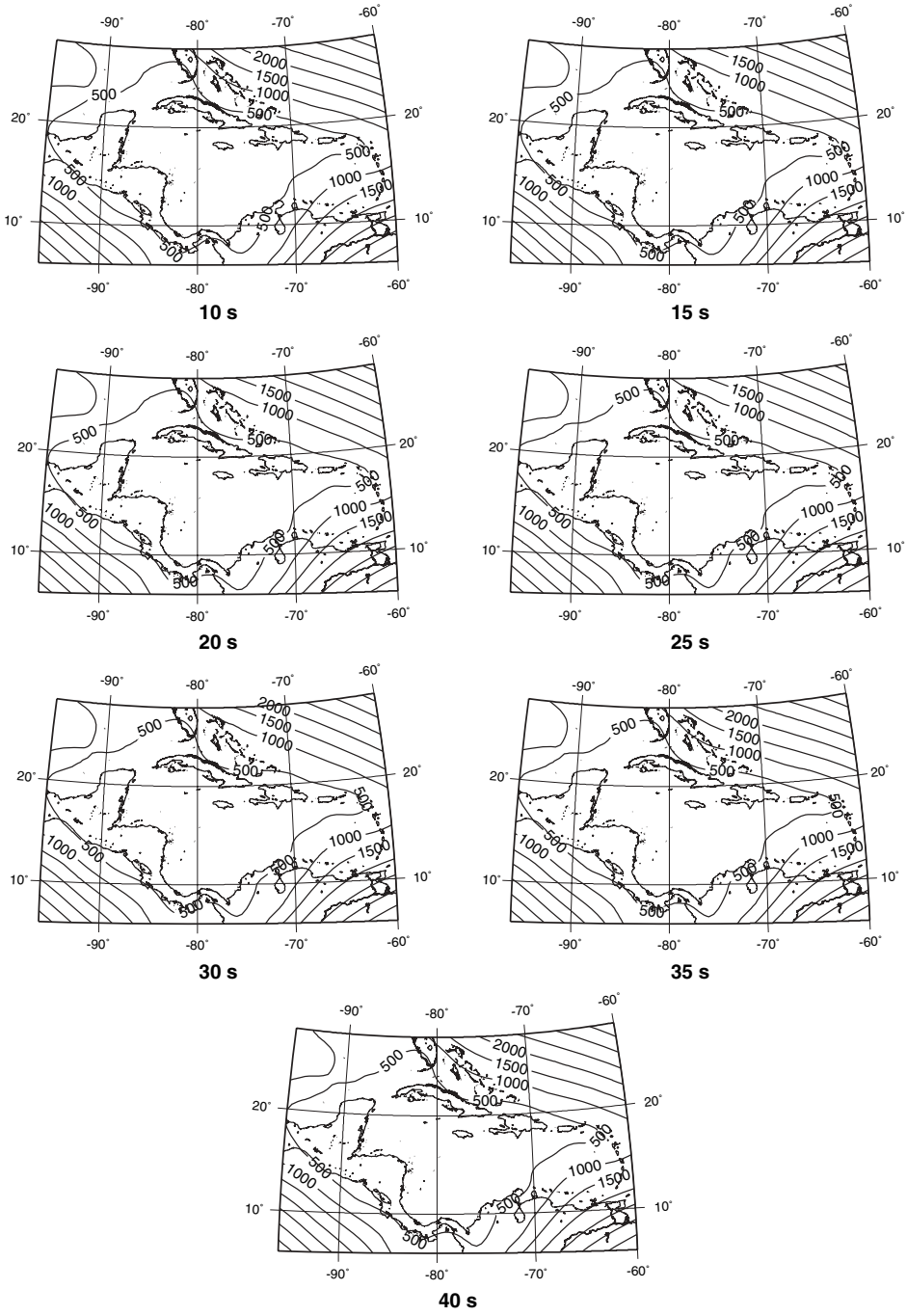

Figure 4
Maps of *a* the horizontal resolution (km) at different periods (10–40 s).

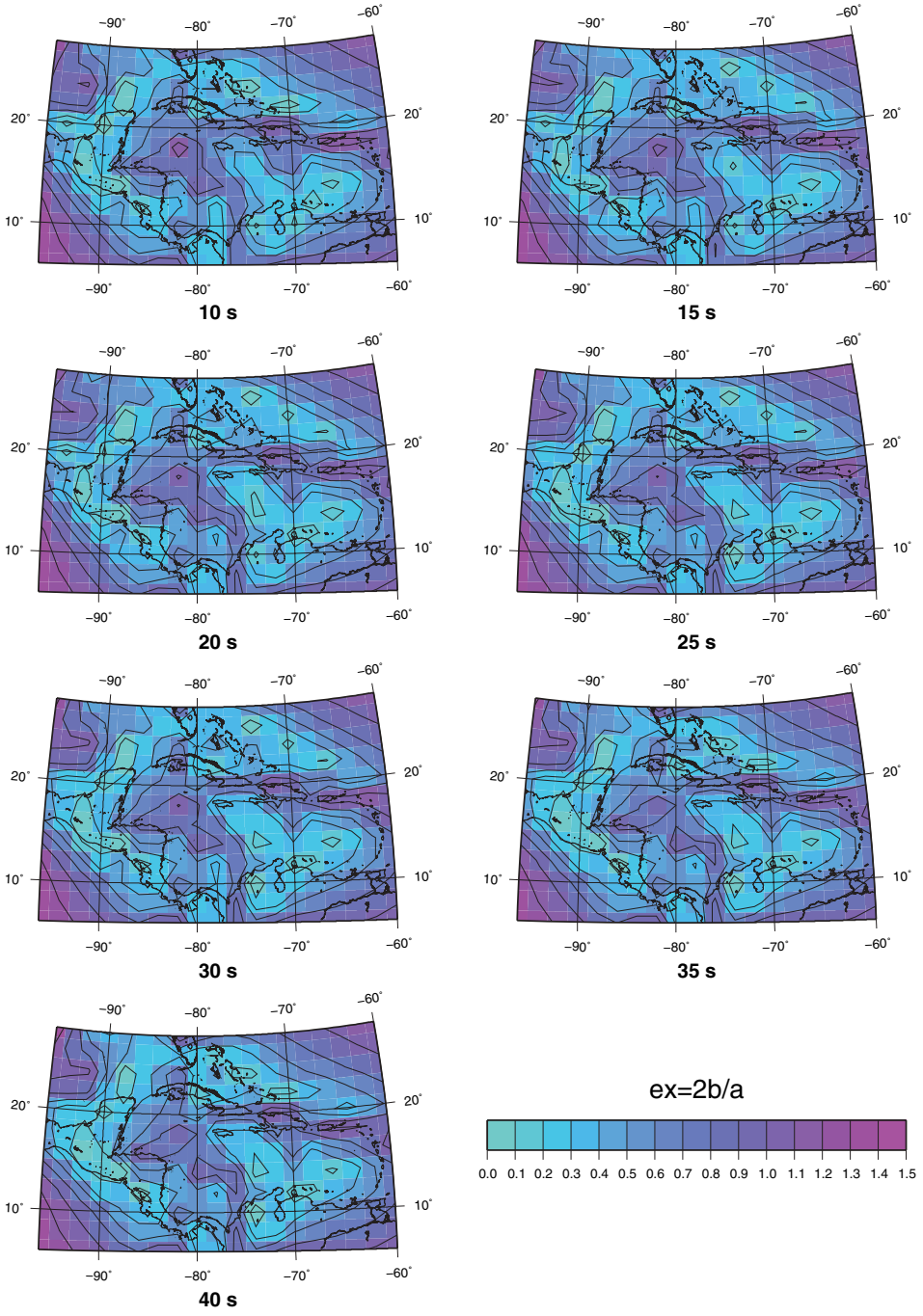

Figure 5
Maps of the azimuthal resolution ex = 2b/a at different periods (10–40 s).

where ε_t is the permitted difference between the values of the variable t (selected as experimental error associated at each period).

- Let $S(O_i, O_j)$ be the similarity function between objects O_i and O_j. Two objects O_i and O_j are β_0-*similar*, if and only if $S(O_i, O_j) \geq \beta_0$, where β_0, the level of the classification, is between 0 and 1. The similarity between objects is calculated by the formula:

$$S(O_i, O_j) = \frac{\sum_{t=1}^{n} p_t \cdot C_t\left[x_t(O_i), x_t(O_j)\right]}{\sum_{t=1}^{n} p_t} \tag{2}$$

where n is the number of considered variables and p_t is the "informative weight" of the variable "t" that may vary between 0 and 1 (selected equal to 0.7 for the period of 10 s. and equal to 1 for all other periods).

- An object belongs to a compact set if the most β_0-*similar* to it belongs to this set too, or if it is the most similar to another object belonging to the set.
- The procedure starts by fixing the β_0-level, then the corresponding β_0-compact sets are determined. This process is made interactively using the procedure described by PICO (1999).

The difference between the informative weight selected for the period $T = 10$ s and the other periods, is due to the fact that this point of the dispersion curves is, in general, the most difficult to determine by FTAN analysis.

The classification of the 81 curves has been made with a similarity level $\beta_0 = 0.51$. This level was selected over a dendrogram, constructed by the program with a trial-and-error procedure, under the condition that the total number of groups formed was of the same order of the main geological features of the analyzed region. As a result of the process, seven groups of dispersion curves are obtained (Fig. 6), which allow us to perform the zoning of the studied region shown in Figure 7. The other group (#8) of dispersion curves (Fig. 6) is formed by those curves which could not be grouped under these conditions of similarity. In the map there is an additional differentiation between regions with the same typical curve, but with significantly different, *a priori* known, geological properties, which allow separate inversion.

c) Determination of the S-wave Velocities vs. Depth Models for the Crust and the Upper Mantle

Due to the nonlinear relationship between the surface wave dispersion and the seismic velocity structure of the Earth, as well as the complexity of the region and the independence of the solutions from the initial models, the nonlinear inversion method called ·hedgehog· (VALYUS, 1968) has been applied to the average dispersion curves for each region. The hedgehog procedure represents a Monte-

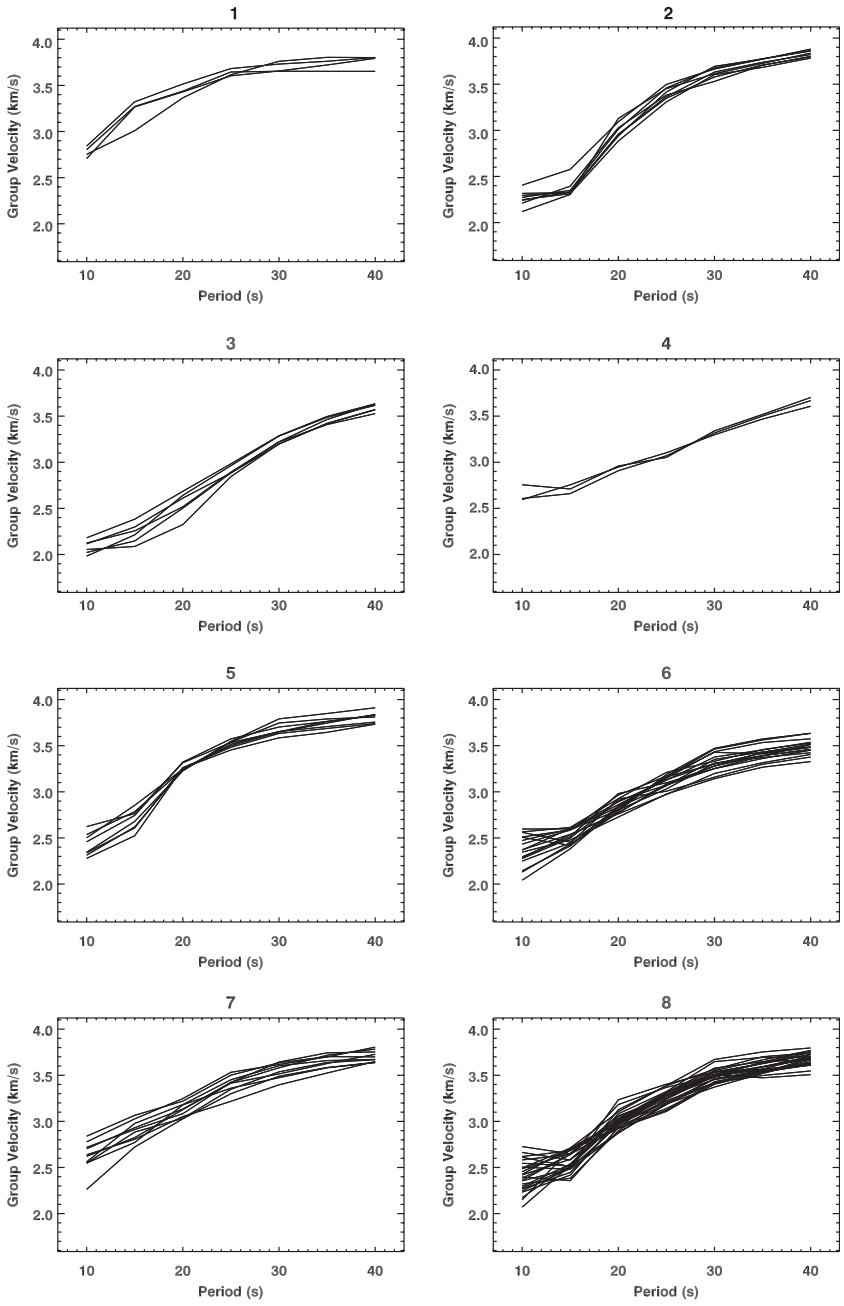

Figure 6
The eight groups of dispersion curves obtained by the classification of the 81 curves with a similarity level $\beta_0 = 0.51$.

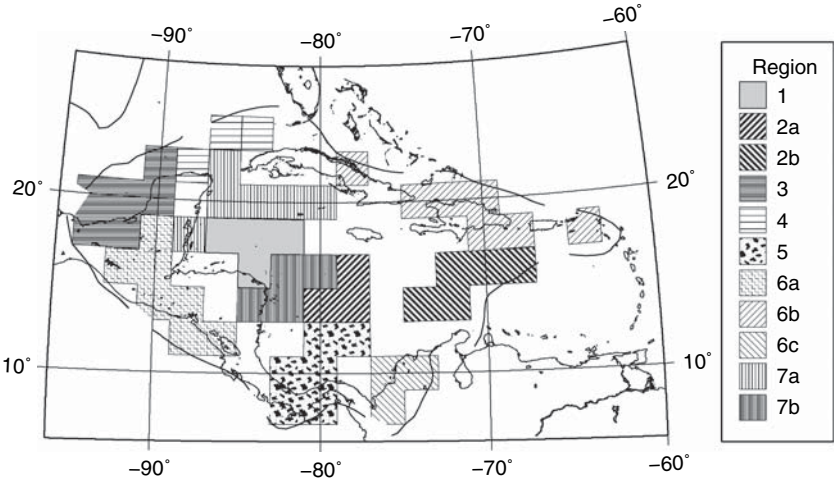

Figure 7
Regionalization scheme: Each region is identified by a different hatching. The regions named by the same number are characterized by the same dispersion curve but different, *a priori* known, properties. Most of the regions are compatible with the resolution length.

Carlo search (to find the velocity vs. depth models consistent with the dispersion curves in a fully nonlinear form) optimized by the use of a guided method that remembers the results of the trials already made, which is not possible in pure Monte-Carlo methods.

The area has been sampled by VDOVIN *et al.* (1999) with a broader-than-our regional scale tomography, using path lengths longer than 4500 km. The density of these paths is lower and the azimuthal distribution is less uniform than in our study, and the determination of geologically meaningful group velocities for periods < 30 sec is questionable over distances of several thousands of km. Therefore we prefer to use our data at the periods for which both data sets are available. Thus we extend our dispersion relations to longer periods, using the group velocity tomographic results of VDOVIN *et al.*, (1999) ranging from 50 sec to 150 sec (Table 3). For each region, the average dispersion curves from each cell in the region were calculated and considered as experimental data. The associated experimental error at each period ($\boldsymbol{\rho}_g$) is determined as the square – root of the sum of the square of the measurement error (between 0.06 and 0.09 km/s depending on the period) and the standard deviation of the group velocity from the average dispersion curve in the region. For each experimental dispersion curve a fraction δ is chosen, usually about 60% of the average of the associated experimental error for all periods. Group velocity curves are computed for each structural model: the model is accepted as a solution (BISWAS and KNOPOFF, 1974; PANZA, 1981) if the difference between the computed and the

Table 3

Experimental data used in the non-linear inversion. For each region and period, group velocity (U), single point error (ρ_g) and r.m.s. values are listed

Period (s)	Region 1		Region 2a		Region 2b		Region 3		Region 4		Region 5	
	U (km/s)	ρ_g (km/s)	U (km/s)	ρ_g (km/s)	U (km/s)	ρ_g (km/s)	U (km/s)	ρ_g (km/s)	U (km/s)	ρ_g (km/s)	U (km/s)	ρ_g (km/s)
10	2.79	0.16	2.27	0.17	2.30	0.09	2.08	0.14	2.65	0.12	2.42	0.15
15	3.23	0.16	2.45	0.16	2.36	0.08	2.23	0.14	2.71	0.09	2.70	0.13
20	3.45	0.09	3.11	0.08	2.98	0.08	2.55	0.14	2.94	0.07	3.26	0.07
25	3.65	0.07	3.47	0.08	3.40	0.08	2.91	0.08	3.08	0.07	3.52	0.07
30	3.71	0.08	3.63	0.08	3.66	0.08	3.24	0.07	3.32	0.06	3.68	0.09
35	3.75	0.09	3.76	0.07	3.76	0.07	3.45	0.07	3.50	0.07	3.74	0.09
40	3.78	0.09	3.86	0.07	3.85	0.07	3.59	0.07	3.66	0.08	3.81	0.09
60	3.86	0.09	3.86	0.08	3.88	0.08	3.80	0.09	3.88	0.09	3.81	0.09
80	3.88	0.09	3.86	0.09	3.84	0.09	3.81	0.10	3.89	0.09	3.83	0.09
100	3.81	0.09	3.81	0.09	3.82	0.09	3.77	0.10	3.85	0.09	3.79	0.09
125	3.73	0.09	3.74	0.09	3.77	0.09	3.74	0.10	3.83	0.09	3.73	0.09
150	3.70	0.09	3.74	0.09	3.76	0.09	3.67	0.10	3.75	0.09	3.72	0.09
δ		0.06		0.057		0.049		0.06		0.050		0.057

Period (s)	Region 6a		Region 6b		Region 6c		Region 7a		Region 7b	
	U (km/s)	ρ_g (km/s)	U (km/s)	ρ_g (km/s)	U (km/s)	ρ_g (km/s)	U (km/s)	ρ_g (km/s)	U (km/s)	ρ_g (km/s)
10	2.24	0.16	2.52	0.11	2.27	0.09	2.58	0.19	2.68	0.15
15	2.48	0.11	2.55	0.11	2.49	0.09	2.87	0.15	2.92	0.13
20	2.80	0.09	2.86	0.09	2.94	0.07	3.14	0.10	3.12	0.10
25	3.08	0.09	3.14	0.09	3.06	0.07	3.38	0.10	3.42	0.09
30	3.28	0.09	3.39	0.09	3.22	0.08	3.52	0.10	3.60	0.08
35	3.39	0.09	3.47	0.09	3.35	0.08	3.61	0.09	3.70	0.07
40	3.46	0.09	3.54	0.09	3.45	0.09	3.69	0.09	3.73	0.08
60	3.77	0.08	3.86	0.09	3.80	0.09	3.84	0.08	3.84	0.08
80	3.78	0.09	3.82	0.09	3.83	0.09	3.89	0.09	3.86	0.09
100	3.75	0.09	3.81	0.09	3.83	0.09	3.84	0.09	3.80	0.09
125	3.70	0.09	3.77	0.09	3.79	0.09	3.78	0.09	3.72	0.09
150	3.67	0.09	3.79	0.09	3.76	0.09	3.73	0.09	3.72	0.09
δ		0.058		0.056		0.051		0.063		0.057

experimental values is less than the measurement error at each period (starting from the largest) and if the r.m.s. value of the differences is less than δ.

The inverted parameters are the thickness of five layers and their Vs velocities, with $Vp/Vs = \sqrt{3}$. The density is fixed at the beginning of the inversion procedure (and remains constant after, due to its low influence on the final results), from its relation with Vp, in rough agreement with the Nafe-Drake relation (GRANT and WEST, 1965; FOWLER, 1995). The parameterization of the input data and the

Table 4

Parameterization used in the nonlinear inversion. Grey area: h (thickness), Vs and Vp of each layer The parameters of the uppermost layers are fixed on the base of available literature [e.g. DENGO et al., 1990; CHULICK and MOONEY, 2002; LIGORRÍA and MOLINA, 1997; MORENO et al., 2002; LASKE and MASTERS, 1997; MOONEY et al., 1998; SMITH and SANDWELL, 1997]. The variable parameters are Pi, with i = 1, … 5 for thickness and i = 6, … 10 for V_s. White area: Step (ΔPi) and a priori allowed variability range for each parameter Pi

Region 1				Region 2a				Region 2b			
H (km)	Vs (km/s)	Vp (km/s)	d (g/cm^3)	h (km)	Vs (km/s)	Vp (km/s)	d (g/cm^3)	h (km)	Vs (km/s)	Vp (km/s)	d (g/cm^3)
0.7	0	1.5	1.03	2.06	0	1.5	1.03	2.55	0	1.5	1.03
0.5	0.72	2.07	1.98	1.0	0.64	2.0	1.95	0.7	0.64	2.0	1.95
2.0	1.93	3.5	2.33	2.8	2.6	4.8	2.6	0.3	1.9	3.4	2.33
P1	P6	P6 × 1.73	2.7	P1	P6	P6 × 1.73	2.5	P1	P6	P6 × 1.73	2.55
P2	P7	P7 × 1.73	2.9	P2	P7	P7 × 1.73	2.6	P2	P7	P7 × 1.73	2.8
P3	P8	P8 × 1.73	3.2	P3	P8	P8 × 1.73	3.15	P3	P8	P8 × 1.73	3.15
P4	P9	P9 × 1.73	3.2	P4	P9	P9 × 1.73	3.2	P4	P9	P9 × 1.73	3.2
P5	P10	P10 × 1.73	3.2	P5	P10	P10 × 1.73	3.2	P5	P10	P10 × 1.73	3.2
h (km)	Step (km)	Range (km)		h (km)	Step (km)	Range (km)		h (km)	Step (km)	Range (km)	
P1	6	8–26		P1	4	5–25		P1	5	5–35	
P2	15	5–35		P2	3	8–26		P2	6	5–23	
P3	20	10–50		P3	24	4–52		P3	16	8–56	
P4	30	20–80		P4	20	15–55		P4	15	15–60	
P5	40	40–160		P5	60	30–150		P5	30	60–120	
Vs (km/s)	Step (km/s)	Range (km/s)		Vs (km/s)	Step (km/s)	Range (km/s)		Vs (km/s)	Step (km/s)	Range (km/s)	
P6	0.3	2.3–4.7		P6	0.2	2.3–3.7		P6	0.03	2.3–3.50	
P7	0.3	3.7–4.3		P7	0.2	2.3–4.15		P7	0.1	3.25–4.15	
P8	0.2	4.3–4.7		P8	0.3	4.1–4.7		P8	0.15	4.15–4.75	
P9	0.25	4.25–4.75		P9	0.2	4.3–4.7		P9	0.2	4.3–4.7	
P10	0.10	4.3–4.7		P10	0.15	4.35–4.75		P10	0.2	4.3–4.7	

determination of the appropriated step (ΔP_i) of each inverted parameter are made following the procedure described by PANZA (1981), and using the code developed by URBAN *et al.* (1993) for the analytical determination of the partial derivatives of the dispersion relations with respect to the structural parameters (Table 4).

A generalization from the available regional and global information is used to fix the parameters of the upper crust and sedimentary layers, while for the water layers, bathymetric information from SMITH and SANDWELL (1997) is used. The structure deeper than 350 km is the same for all the considered cells and is defined accordingly with already published models, e.g. MONTAGNER and KENNET (1996) and DU *et al.* (1998).

To reduce the effects of the projection of possible systematic errors into the inverted structural model, we choose for each region the solution with the r.m.s. as close as possible to the average value of the r.m.s. of all the solutions for the region. If

Table 4

(Contd.)

Region 3				Region 4				Region 5			
h (km)	Vs (km/s)	Vp (km/s)	d (g/cm^3)	h (km)	Vs (km/s)	Vp (km/s)	d (g/cm^3)	h (km)	Vs (km/s)	Vp (km/s)	d (g/cm^3)
0.1	0	1.5	1.03	0.1	0	1.5	1.03	1.8	0	1.5	1.03
1.5	0.92	2.25	2.02	0.4	1.2	2.4	2.1	1.4	0.9	2.36	1.96
2.5	2.08	3.75	2.37	1.0	1.93	3.4	2.33	2.8	1.8	4.4	2.33
P1	P6	P6 × 1.73	2.5	P1	P6	P6 × 1.73	2.7	P1	P6	P6 × 1.73	2.65
P2	P7	P7 × 1.73	2.9	P2	P7	P7 × 1.73	2.7	P2	P7	P7 × 1.73	3.2
P3	P8	P8 × 1.73	3.15	P3	P8	P8 × 1.73	3.2	P3	P8	P8 × 1.73	3.21
P4	P9	P9 × 1.73	3.2	P4	P9	P9 × 1.73	3.22	P4	P9	P9 × 1.73	3.2
P5	P10	P10 × 1.73	3.2	P5	P10	P10 × 1.73	3.2	P5	P10	P10 × 1.73	3.2
h (km)	Step (km)	Range (km)		h (km)	Step (km)	Range (km)		h (km)	Step (km)	Range (km)	
P1	3	5–23		P1	4	5–25		P1	4	5–25	
P2	12	6–42		P2	4	5–25		P2	20	10–30	
P3	10	11–31		P3	5	7–32		P3	20	10–50	
P4	15	15–30		P4	20	5–45		P4	25	15–65	
P5	30	60–120		P5	30	60–150		P5	60	60–120	
Vs (km/s)	Step (km/s)	Range (km/s)		Vs (km/s)	Step (km/s)	Range (km/s)		Vs (km/s)	Step (km/s)	Range (km/s)	
P6	0.1	2.3–3.7		P6	0.2	2.3–4.7		P6	0.1	2.3–4.3	
P7	0.2	3.7–4.1		P7	0.2	2.3–4.7		P7	0.3	4.2–4.8	
P8	0.2	4.1–4.7		P8	0.2	4.3–4.7		P8	0.15	4.25–4.7	
P9	0.2	4.3–4.7		P9	0.2	4.25–4.85		P9	0.25	4.25–4.75	
P10	0.2	4.3–4.7		P10	0.2	4.3–4.7		P10	0.25	4.25–4.75	

more than one solution satisfies this "average r.m.s." criterion, the one with the most frequent ΔP_i is selected.

Discussion

The tomographic maps (Fig. 3) evidence the geotectonic heterogeneity of the Caribbean region, as it was expected from *a priori* knowledge (DENGO and CASE, 1990; PINDELL and KENNAN, 2001). Both the tomographic maps and the structural models obtained as a result of the inversion (Table 5) indicate a predominance of oceanic-like crust, with evidence for other crustal types in some parts of the studied region.

Region 1 (Figs. 7 and 8), which comprises the Cayman Trough, evidences an oceanic type of crust with a Moho at a depth of about 15 km. The upper mantle shear-wave velocity, in the range 4.15–4.3 km/s, points towards the presence of a young ocean (LEEDS *et al.*, 1974; FORSYTH, 1975; PANZA, 1980). This result is in very good agreement with the results of previous investigations based on different

Table 4

(Contd.)

Region 6a				Region 6b				Region 6c			
h (km)	Vs (km/s)	Vp (km/s)	d (g/cm3)	h (km)	Vs (km/s)	Vp (km/s)	d (g/cm^3)	h (km)	Vs (km/s)	Vp (km/s)	d (g/cm^3)
0.6	1.0	2.4	2.05	1.6	0	1.5	1.03	0.9	1.09	2.4	2.08
0.6	1.2	2.5	2.1	0.6	0.84	2.05	1.97	1.5	2.18	3.95	2.18
5.0	3.0	5.19	2.5	2.4	1.93	3.45	2.33	4.0	3.0	5.19	2.5
P1	P6	P6 × 1.73	2.85	P1	P6	P6 × 1.73	2.5	P1	P6	P6 × 1.73	2.6
P2	P7	P7 × 1.73	2.8	P2	P7	P7 × 1.73	2.7	P2	P7	P7 × 1.73	2.85
P3	P8	P8 × 1.73	3.2	P3	P8	P8 × 1.73	2.95	P3	P8	P8 × 1.73	3.2
P4	P9	P9 × 1.73	3.2	P4	P9	P9 × 1.73	3.2	P4	P9	P9 × 1.73	3.2
P5	P10	P10 × 1.73	3.2	P5	P10	P10 × 1.73	3.2	P5	P10	P10 × 1.73	3.2
h	Step	Range		h	Step	Range		h	Step	Range	
(km)	(km)	(km)		(km)	(km)	(km)		(km)	(km)	(km)	
P1	4	6–18		P1	8	6–22		P1	3	5–23	
P2	15	5–35		P2	6	7–31		P2	10	10–40	
P3	30	22–82		P3	20	3.5–43.5		P3	15	10–55	
P4	50	27.5–77.5		P4	30	17.5–77.5		P4	20	17.5–57.5	
P5	50	30–130		P5	45	60–150		P5	40	40–120	
Vs	Step	Range		Vs	Step	Range		Vs	Step	Range	
(km/s)	(km/s)	(km/s)		(km/s)	(km/s)	(km/s)		(km/s)	(km/s)	(km/s)	
P6	0.1	3.0–4.7		P6	0.1	2.35–3.75		P6	0.2	3.0–3.4	
P7	0.3	3.15–4.35		P7	0.2	3.15–3.95		P7	0.3	3.15–4.65	
P8	0.2	4.3–4.7		P8	0.3	3.9–4.5		P8	0.2	4.3–4.7	
P9	0.2	4.3–4.7		P9	0.2	4.3–4.7		P9	0.2	4.3–4.7	
P10	0.2	4.3–4.7		P10	0.1	4.3–4.7		P10	0.2	4.3–4.7	

geophysical methods (e.g., DENGO and CASE, 1990; TEN *et al.*, 2001). In region 5 (Figs. 7 and 8), that corresponds to part of the Colombian Basin and north of the Panama Deformed Belt, the crust is oceanic, the Moho depth being at about 18 km with an average Vs above about 3.6 km/s, typical of the lower crust. This crustal thickness, anomalously large for a standard oceanic crust, could be an indication of the presence of a type of accretionary crust, mainly present in the Panama Deformed Belt (DENGO and CASE, 1990). The upper mantle velocity in the range 4.35–4.65 km/s suggests that here the ocean is older than in the Cayman Trough. In both oceanic regions a slight low velocity channel can be present in the mantle.

Regions 2a (comprised of the southern Nicaraguan Rise) and 2b (including parts of the Venezuelan Basin and Beata Ridge; Figs. 7 and 8) are characterized by the same type of dispersion curve. In both cases a crust of oceanic type (thickened) is present, the Moho depth is in the range 20–30 km, the upper mantle shear velocity can be as high as 4.7 km/s and a low velocity channel in the mantle, starting at depths in the range 55–75 km, talks about an aged oceanic crust (PANZA, 1980). In both regions two crustal layers are present, one of them, the thicker, with a velocity

Table 4

(Contd.)

Region 7a				Region 7b			
h (km)	Vs (km/s)	Vp (km/s)	d (g/cm^3)	h (km)	Vs (km/s)	Vp (km/s)	d (g/cm^3)
2.5	0	1.5	1.03	1.2	0	1.5	1.03
0.7	1.1	2.3	2.3	1.3	0.84	3.1	1.95
1.3	2.7	5.1	2.7	3.0	2.4	5.5	2.5
P1	P6	P6 × 1.73	2.7	P1	P6	P6 × 1.73	2.65
P2	P7	P7 × 1.73	3.1	P2	P7	P7 × 1.73	3.1
P3	P8	P8 × 1.73	3.2	P3	P8	P8 × 1.73	3.2
P4	P9	P9 × 1.73	3.2	P4	P9	P9 × 1.73	3.2
P5	P10	P10 × 1.73	3.2	P5	P10	P10 × 1.73	3.2
h	Step	Range		h	Step	Range	
(km)	(km)	(km)		(km)	(km)	(km)	
P1	10	5–35		P1	6	11–35	
P2	15	15–45		P2	10	15–35	
P3	30	15–45		P3	40	15–55	
P4	40	25–65		P4	40	15–55	
P5	60	60–120		P5	60	30–150	
Vs	Step	Range		Vs	Step	Range	
(km/s)	(km/s)	(km/s)		(km/s)	(km/s)	(km/s)	
P6	0.2	2.45–4.25		P6	0.15	2.35–4.3	
P7	0.3	4.0–4.6		P7	0.2	4.0–4.6	
P8	0.2	4.3–4.7		P8	0.2	4.3–4.7	
P9	0.2	4.3–4.7		P9	0.2	4.3–4.7	
P10	0.2	4.3–4.7		P10	0.2	4.3–4.7	

ranging from 3.45 to 3.65 km/s, the other in region 2a represents a thin upper crust layer and in region 2b a thin crustal low velocity channel. CHULICK and MOONEY (2002) give a thinner crust, however the difference between our values and their values is well within the uncertainties and an aged oceanic crust can well be about 20-km thick. Regions 6a, 6b and 6c (Figs. 7 and 8) are located in geological provinces where mainly an accretionary crust is present (DENGO and CASE, 1990).

In region 6a, coinciding with the Central American accretionary complex and with part of the Chortis Block and Maya Block of Central America (the last two blocks have been identified as continental by DENGO and CASE, (1990), the Moho depth ranges 27–45 km, while in regions 6b and 6c it ranges 22–33 km. In region 6b, coinciding with the complex accretionary type of crust present in the Greater Antilles Deformed Belt, there is a low velocity channel in the crust, while the upper mantle properties are consistent with the presence of lithospheric roots extending to depths exceeding 200 km. Region 6c, included in the South Caribbean-northern South America accretionary complexes (DENGO and CASE, 1990), is characterized by a fairly deep low velocity channel in the mantle, indicating that the lithospheric roots

Table 5

*Range of variability of the parameters h (thickness) and Vs for each layer of the chosen solution. (Grey area evidences fixed parameters). In the table the values of the inverted parameters are rounded off to 0.5 km or to 0.05 km/s. We take into account the a priori information used to constrain the inversion, therefore, for each parameter, the chosen value does not necessarily fall in the center of the variability range that can turn out to be smaller than the step,? ΔPi, used in the inversion. The thickness marked by * is not a truly inverted parameter, but it satisfies the condition that the total thickness from the free surface to the top of the fixed upper mantle is equal to a predefined quantity H. In this study H = 350 km. The structure deeper than H is the same for all the considered cells and it has been fixed accordingly with already published models [MONTAGNER and KENNET, 1996; DU et al., 1998]*

Region 1		Region 2a		Region 2b		Region 3	
h (km)	Vs (km/s)	h (km)	Vs (km/s)	h (km)	Vs (km/s)	h (km)	Vs (km/s)
0.7	0	2.06	0	2.55	0	0.1	0
0.5	0.72	1.0	0.64	0.7	0.64	1.5	0.92
2.0	1.93	2.8	2.6	0.3	1.9	2.5	2.08
11–17	3.75–4.05	5–7	3.3–3.5	12.5–17.5	3.45–3.5	15.5–18.5	3.25–3.35
12.5–27.5	4.15–4.3	9.5–12.5	3.45–3.65	5–8	3.2–3.3	6–12	3.8–4.0
40–50	4.4–4.6	40–52	4.55–4.7	32–48	4.65–4.75	26–31	4.4–4.6
20–35	4.25–4.40	45–55	4.4–4.6	37.5–52.5	4.4–4.6	22.5–37.5	4.6–4.7
140–160	4.45–4.55	120–150	4.45–4.6	105–120	4.4–4.6	75–105	4.3–4.4
*	4.75	*	4.75	*	4.75	*	4.75
67	4.9	67	4.9	67	4.9	67	4.9

Region 4		Region 5		Region 6a		Region 6b	
h (km)	Vs (km/s)	h (km)	Vs (km/s)	h (km)	Vs (km/s)	h (km)	Vs (km/s)
0.1	0	1.8	0	0.6	1.0	1.6	0
0.4	1.2	1.4	0.9	0.6	1.2	0.6	0.84
1.0	1.93	2.8	1.8	5.0	3.0	2.4	1.93
11–15	3.2–3.4	11–15	3.65–3.75	8–12	3.05–3.15	10–18	3.6–3.7
15–19	3.7–3.9	10–20	4.35–4.65	12.5–27.5	3.9–4.2	7–10	3.25–3.45
15–20	4.3–4.4	40–50	4.5–4.65	67–82	4.4–4.6	13.5–33.5	4.35–4.5
35–45	4.55–4.75	52.5–65	4.4–4.65	52.5–77.5	4.6–4.7	62.5–77.5	4.4–4.6
135–150	4.4–4.6	90–120	4.4–4.65	55–105	4.3–4.4	127.5–150	4.55–4.65
*	4.75	*	4.75	*	4.75	*	4.75
67	4.9	67	4.9	67	4.9	67	4.9

may reach here about 200 km of depth. In the three regions two crustal layers are present. In regions 6a and 6c, that contain the Cocos-Caribbean and South Caribbean subduction zones, respectively, the Vs in the lower one ranges from 3.6 km/s to 4.2 km/s.

In region 3 (Figs. 7 and 8), which is contained in the Maya Block, the Moho depth ranges 26–35 km and points toward the presence of a (possibly thickened) continental type of crust. In region 4 (Figs. 7 and 8), in the eastern part of the Maya Block, the Moho depth ranges 27.5–35.5 km, in agreement with the presence of continental crust in this geological province. In both regions two well distinct, upper

Table 5

(Contd.)

Region 6c		Region 7a		Region 7b	
h (km)	Vs (km/s)	h (km)	Vs (km/s)	h (km)	Vs (km/s)
0.9	1.09	2.5	0	1.2	0
1.5	2.18	0.7	1.1	1.3	0.84
4.0	3.0	1.3	2.7	3.0	2.4
6.5–9.5	3.1–3.3	10–20	3.55–3.75	14–20	3.65–3.8
10–15	3.6–3.9	22.5–37.5	4.15–4.45	15–20	4.3–4.5
32.5–47.5	4.3–4.4	30–45	4.4–4.6	35–55	4.4–4.6
47.5–57.5	4.6–4.7	45–65	4.4–4.6	15–35	4.6–4.7
60–100	4.3–4.4	60–90	4.3–4.4	60–120	4.3–4.4
*	4.75	*	4.75	*	4.75
67	4.9	67	4.9	67	4.9

and lower crustal layers are identified and a wide low velocity channel in the mantle is present, starting at depths ranging from approximately 70 km to 100 km, as could be expected in a stable continental platform (PANZA, 1981).

The Eastern Nicaraguan Rise comprises region 7b (Figs. 7 and 8): the presence of a thickened oceanic type of crust is consistent with a Moho depth ranging from 19.5 km to 25.5 km and with the presence of a well developed low velocity channel in the upper mantle, while in region 7a (Figs. 7 and 8; Yucatan Basin, parts of the Cayman Trough and Greater Antilles accretionary complex) the Moho depth ranges 14.5–24.5 km, with a lowest upper mantle velocity ranging from 4.1 km/s to 4.45 km/s and a lower crust velocity (3.55–3.75 km/s). The features shown in 7a are well consistent with previous results from seismic profiles studies (CHULICK and MOONEY, 2002).

Other curves, which were grouped as type 8 by the logical-combinatorial procedure, did not determine any specific region; therefore they have not been inverted.

Conclusions

1. The tomographic study of the group velocity of the fundamental mode of Rayleigh waves ranging from 10 to 40 seconds in the Central-West Caribbean improves our knowledge of the crust and upper mantle properties of this region, and evidences its heterogeneity and the predominant presence of oceanic-like crust.
2. Eleven regions have been identified on the basis of the similarity of their group velocity dispersion properties. For each region the structure of the crust and upper mantle, as obtained by nonlinear inversion of extended dispersion curves until 150 s, is described by S-waves velocity vs. depth models.

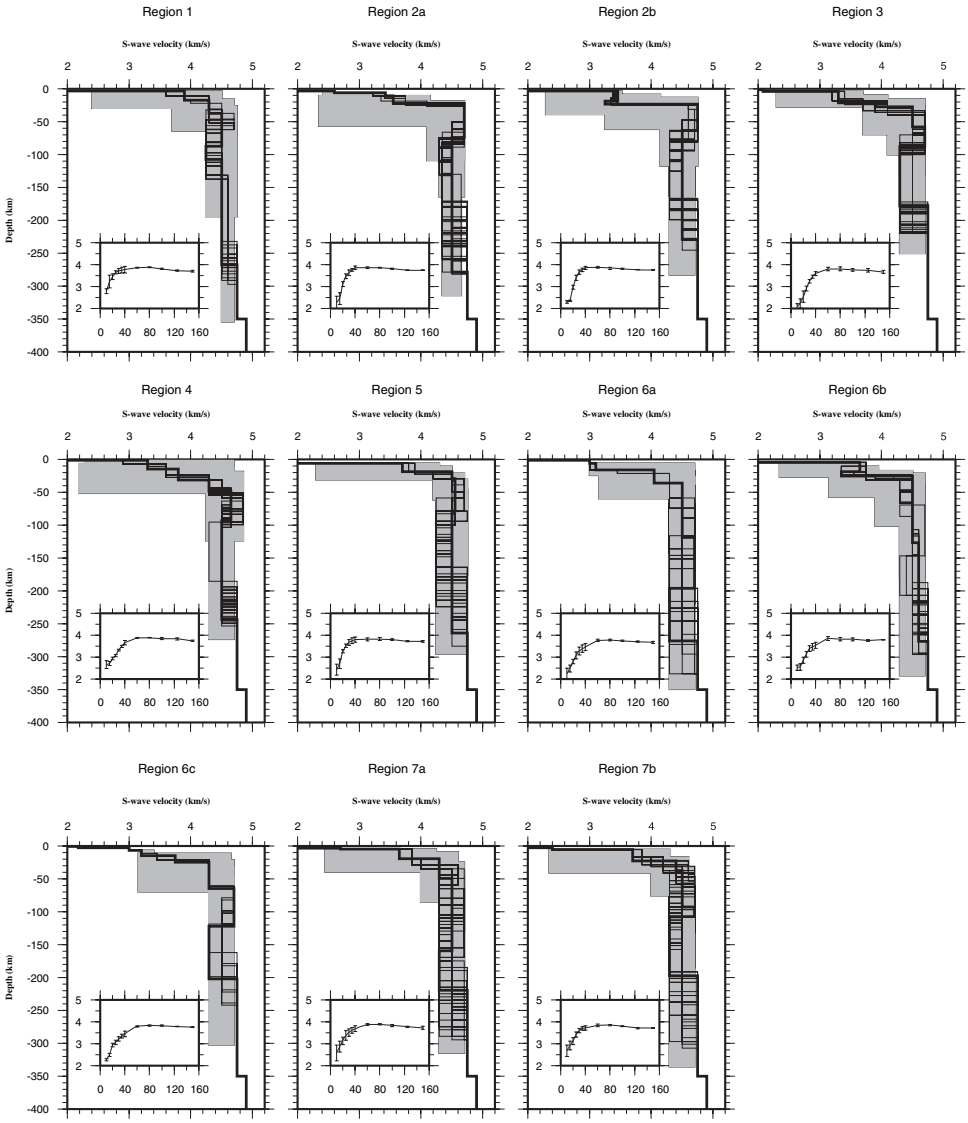

Figure 8

The set of solutions (the S-wave velocity as a function of depth) obtained from the nonlinear inversion for all the regions. A representative structural solution (see text for details) is shown by a bold line and the shaded area is the portion of the parameter space explored during the inversion. In each smaller frame, the group velocity values corresponding to the representative model are compared with the experimental values and their error bars.

3. In the regions 1, 2a, 2b, 5, 7a and 7b the crust and upper mantle structure is of oceanic type, and indicate, in agreement with the average models of (LEEDS *et al.*, 1974; FORSYTH, 1975; PANZA, 1981), the presence of oceans of different age

(PANZA, 1981). A single layer oceanic crust is detected in all regions, with the exception of regions 2a and 2b where an additional very thin layer is present.

4. Regions 3 and 4 have the properties of stable continental structures.
5. Regions 6b and 6c are located over the major geological zones of the accretionary crust of the Caribbean region and are characterized by a peculiar crust and upper mantle structure, indicating the presence of lithospheric roots reaching, at least, about 200 km depth.

Acknowledgement

The authors express thanks to Anatoli L. Levshin from the University of Colorado, for kindly gently providing us with the long-period group velocities available at CIEI, University of Colorado at Boulder and to Giordano Chimera for the careful assistance in part of the data processing. They also recognize the help of Enrique Diego Arango Arias, from the National Centre for Seismological Research of Cuba in the geological interpretation of the results, the two anonymous reviewers and the editor J. Arthur Snoke for their comments that substantially improved this paper. The present work is done with the financial support of the Associateship and TRIL Programs and ESP (SAND group) Section of the ''Abdus Salam'' International Centre for Theoretical Physics, of the Ministry of Science, Technology and Environment of Cuba, as well as founded by the Italian MIUR Cofin-2001 (2001045878_007), Cofin-2002 (2002047575_002) and the Italian Programma Nazionale di Ricerche in Antartide (PNRA) 2004-2006, project 2.7–2.8 (''Sismologia a larga banda nella regione del Mare di Scotia e suo utilizzo per lo studio della geodinamica della litosfera''). Additional financial support was obtained from the UNESCO/IGCP Project 487 and ICTP Network NET-58 ''Seismic microzoning in Latina American cities''.

Appendix A

Frequency Time Analysis (FTAN) Original seismogram (Input file). FTAN map with the corresponding dispersion curve. Resulting seismogram with the fundamental mode of the Rayleigh surface waves (Output file).

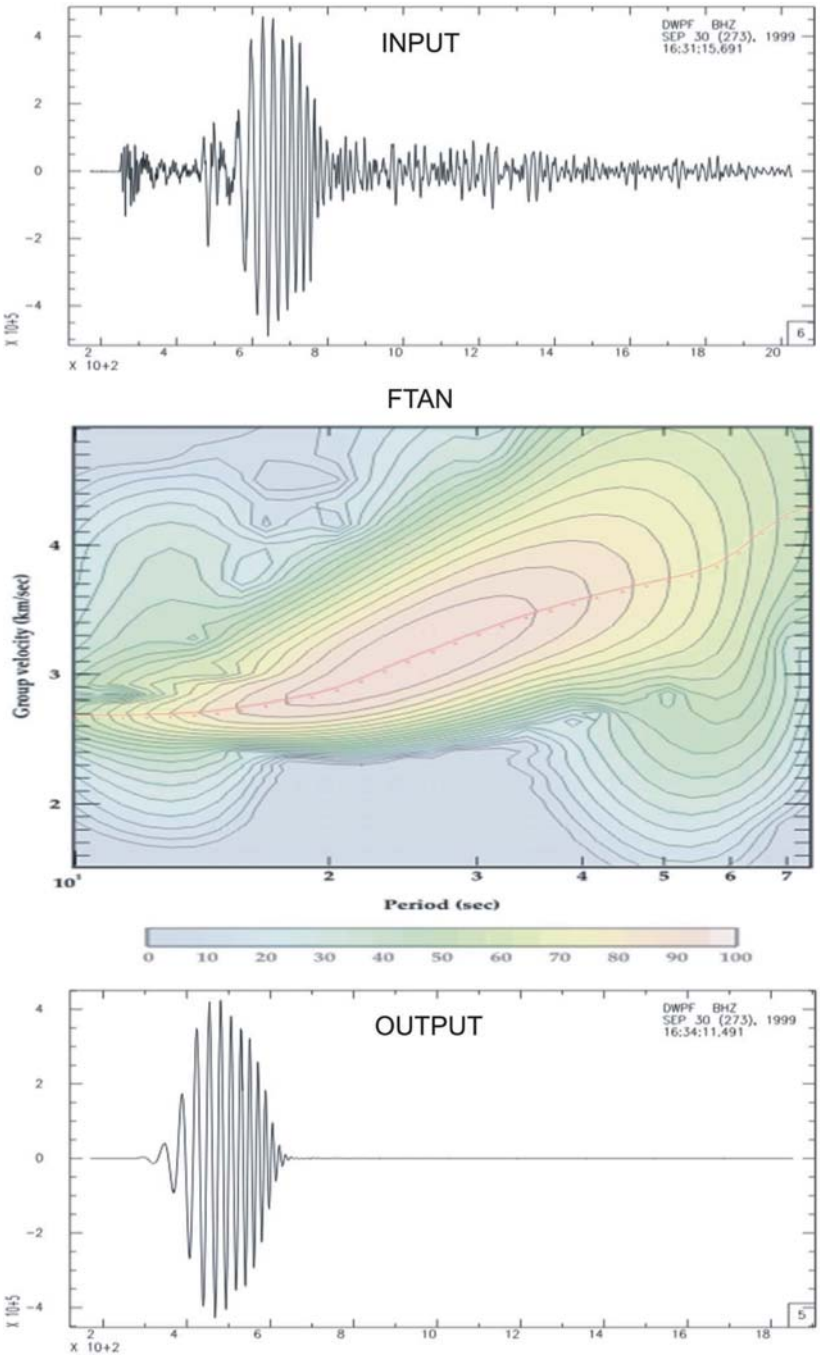
INPUT
DWPF BHZ
SEP 30 (273), 1999
16:31:15.691
X 10+5
X 10+2
FTAN
Group velocity (km/sec)
Period (sec)
OUTPUT
DWPF BHZ
SEP 30 (273), 1999
16:34:11.491

Reference

Álvarez, L. (1977), *Dispersión de la velocidad de grupo de las ondas de Rayleigh en la región del Caribe*, Informe Científico-Técnico No. 5, Instituto de Geofísica y Astronomía, La Habana, Cuba.

Backus, G.E. and Gilbert, F. (1968), *The resolving power of gross earth data,* Geophys. J. *16*, 169–2005.

Backus, G.E. and Gilbert, F. (1970), *Uniqueness in the inversion of inaccurate gross earth data,* Philos. Trans. R. Soc. Lond. *266*, 123–192.

Bassin, C., Laske, G., and Masters, G. (2000), *The current limits of resolution for Surface wave tomography in North America*, EOS Trans. AGU *81*, F897.

Biswas, N.N. and Knopoff, L. (1974), *The structure of the upper mantle under the U.S. from the dispersion of Rayleigh waves,* Geophys. J. R. Astr. Soc. *36*, 515–539.

Chulick, G.S. and Mooney, W.D. (2002), *Seismic structure of the crust and uppermost mantle of North America and adjacent oceanic basins: A synthesis*, Bull. Seism. Soc. Am. *92*(6), 2478–2492.

Dengo, G. and Case, J.E., *The Geology of North America. Volume H. The Caribbean Region* (The Geolog. Soc. Am., Boulder, U.S.A, 1990).

Ditmar, P.G. and Yanovskaya, T.B. (1987), *A generalization of the Backus-Gilbert method for estimation of lateral variations of surface wave velocity*, Izv. Akad. Nauk SSSR, Fizika Zemli (6), 30–60.

Du, Z.J., Michelini, A., and Panza, G.F. (1998), *EurID: A regionalised 3-D seismological model of Europe,* Phys. Earth Planet. Inter. *105*, 31–62.

Forsyth, D.A. (1975), *The early structural evolution and anisotropy of the oceanic upper mantle,* Geophys. J. R. ASTR. Soc. *43*, 103–162.

Fowler, C.M.R., *The Solid Earth. An Introduction to Global Geophysics* (Cambridge Univ. Press 1995).

González, O., Álvarez, L., Panza, G.F., and Chimera, G., *Modelos de corteza de la región del Caribe a partir de la dispersión de ondas superficiales*. In *Sismicidad de Cuba y estructura de la corteza en el Caribe* pp. 45–56 (Editorial Academia, La Habana, Cuba, 2000).

Grant, F.S. and West G.F., *Interpretation Theory in Applied Geophysics* (McGraw-Hill Inc., New York, U.S.A, 1965).

Laske, G. and Masters, G. (1997), *A global digital map of sediment thickness*, EOS Trans. AGU *78*, F483.

Leeds, A.R., Knopoff, L., and Kausel, E.G. (1974), *Variations of upper mantle structure under the Pacific Ocean,* Science *186*, 141–143.

Levshin, A.L., Pisarenko, V.F., and Pogrebinsky, G.A. (1972), *On a frequency-time analysis of oscillations*, Ann. Geophys. *28*(2), 211–218.

Levshin, A.L., Radnikova, L.I., and Berger, J. (1992), *Peculiarities of surface wave propagation across Central Eurasia*, Bull. Seismol. Soc. Am. *82*, 2464–2493.

Levshin, A.L., Ritzwoller, M.H., and Resovsky, J.S. (1999), *Source effects on surface wave travel times and group velocity maps,* Phys. Earth Planet. Inter. *115*, 293–312.

Ligorría, J.P. and Molina, E. (1997), *Crustal velocity structure of Southern Guatemala using refracted and Sp converted waves*, Geofísica Intern. *36*(1).

Montagner, J.P. and Kennet, B.L.N. (1996), *How to reconcile body-wave and normal-mode reference Earth models*, Geophys. J. Int. *125*, 229–248.

Mooney, W.D., Laske, G., and Masters, T.G. (1998), *CRUST 5.1: A global crustal model at* $5^\circ \times 5^\circ$, J. Geophys. Res. *103*(B1), 727–747.

Moreno, B., Grandison, M., and Atakan, K. (2002), *Crustal velocity model along the Southern Cuban margin: Implications for the tectonic regime at an active plate boundary,* Geophys. J. Int. *151*, 632–645.

Panza, G.F., *Evolution of the Earth's lithosphere. NATO Adv. Stud. Inst. Newcastle, 1979*. In *Mechanisms of Continental Drift and Plate Tectonics* (P.A. Davies and S.K. Runcorn, ed.) pp. 75–87 (Academic Press, 1980).

Panza, G.F., *The Resolving power of seismic surface waves with respect to crust and upper mantle structural models,* In *The Solution of the Inverse Problem in Geophysical Interpretation* (Cassinis, R. ed.) pp. 39–77. (Plenum Publ. Corp. 1981)

Panza, G.F., Mueller, S.T., and Calcagnile, G. (1980), *Three gross features of lithosphere-astenosphere system in Europe from seismic surface waves and body waves*, Pure and Appl. Geophys. *118*, 1209–1212.

Papazachos, B.C. (1964), *Dispersion of Rayleigh waves in the Gulf of Mexico and Caribbean Sea*, Bull. Seismol. Soc. Am. *54*(3), 909–926.

PICO, R. (1999), *Determinación del umbral de semejanza β_0 para los algoritmos de agrupamiento lógico-combinatorios, mediante el dendrograma de un algoritmo jerárquico,* SIARP'99, IV Simposio Iberoamericano de Reconocimiento de Patrones. Memorias, 259–265.

PINDELL, J. and KENNAN, L., *Kinematic evolution of the Gulf of Mexico and Caribbean*. In *GCSSEPM Research Conference* (R. Fillon, ed.) (Houston, U.S.A. 2001).

RUIZ, J., PICO, R., LÓPEZ, R., ALAMINOS, C., LAZO, M., BAGGIANO, M., BARRETO, E., SANTANA, A., ALVAREZ, L., and CHUY, T. (1992), *PROGNOSIS y sus aplicaciones a las geociencias,* In *IBERAMIA-92*, III Congreso Iberoamericano de Inteligencia Artificial, Memorias. México: LIMUSA, pp. 561–586.

SANTO, T. (1967), *Lateral variation of rayleigh waves dispersion character. Part IV: The Gulf of Mexico and Caribbean Sea*, Bull. Earthq. Res. Inst. *45*(4), 963.

SMITH, W.H.F. and SANDWELL, D.T. (1997), *Global sea floor topography from satellite altimetry and ship depth soundings*, Sci Magaz *277*, issue 5334.

TARR, A.C. (1969), *Rayleigh waves dispersion in the North Atlantic Ocean, Caribbean Sea and the Gulf of Mexico*, J. Geophys. Res. *74*(6), 1591.

TEN BRINK, U.S., COLEMAN, D.F., and DILLON, W.P (2001), *Asymmetric sea-floor spreading, crustal thickness variations and transitional crust in Cayman Trough from gravity* [abs.], Geolog. Soc. Am., Abstracts with Programs, Annual Meeting, Boston, U.S.A *33*(6), A154.

URBAN, L., CICHOWICZ, A., and VACCARI, F. (1993), *Computation of analytical partial derivatives of phase and group velocities of Rayleigh waves respect to structural parameters,* Studia Geoph. Geod. *36*, 14–36.

VALYUS, V.P. (1968), *Determining seismic profiles from a set of observations* (in Russian), Vychislitielnaya Seismologiya *4*, 3–14. English translation: *Computational Seismology* (V.I. Keylis-Borok, ed.) pp. 114–118, (Consultants Bureau, 1972).

VAN DER HILST, R. D. (1990), *"Tomography with P, PP and pP Delay-time Data and the Three-dimensional Mantle Structure below the Caribbean Region"*, Ph.D. Thesis, University of Utrecht, The Netherlands.

VDOVIN, O., RIAL, J.A., LEVSHIN, A.L., and RITZWOLLER, M.H. (1999), *Group-velocity tomography of South America and the surrounding oceans,* Geophys. J. Int. *136*, 324–340.

YANOVSKAYA, T.B. (1997), *Resolution estimation in the problems of seismic ray tomography*, Izvestiya, Physics of the Solid Earth *33*(9), 762–765.

WU, F.T. and LEVSHIN, A. (1994), *Surface-wave group velocity tomography of east Asia,* Phys. Earth Planet Int. *84*, 59–77.

YANOVSKAYA, T.B. and DITMAR, P.G. (1990), *Smoothness criteria in surface wave tomography*, Geophys. J. Int. *102*, 63–72.

ZAPATA, J.A., GUASCH, F., SERRANO, M., MONTENEGRO, C., DIEZ, E.R., GONZÁLEZ, O.F., and DEL PINO, J.R. (2001), *Servicio Sismológico Nacional de Cuba: Primeros resultados después de la transformación tecnológica.* In *Red de estaciones e investigaciones sismológicas en Cuba*, Editorial Academia, La Habana, Cuba, pp. 27–34.

(Received August 2, 2004, accepted February 2, 2007)
Published Online First: July 4, 2007